Malays J Pathol 2026; 48(1): 37 – 52

ORIGINAL ARTICLE

Intestinal barrier dysfunction and differential *CLDN8* and *MUC1* expression in vedolizumab responsiveness among inflammatory bowel disease patients: a proof-of-concept study

Nurul Aqilah SHAHABUDIN[1], Raja Affendi RAJA ALI[2,3,6], Geok Chin TAN[4], Norfilza Mohd MOKHTAR[5]*

[1]Department of Physiology, Faculty of Medicine, Universiti Kebangsaan Malaysia, Cheras, Kuala Lumpur 56000, Malaysia; [2]GUT Research Group, Faculty of Medicine, Universiti Kebangsaan Malaysia, 56000 Cheras, Kuala Lumpur, Malaysia; [3]Sir Jeffery Cheah Sunway Medical School, School of Medical and Life Sciences, Sunway University, 47500 Sunway City, Selangor, Malaysia; [4]Department of Pathology, Faculty of Medicine, Universiti Kebangsaan Malaysia, 56000 Cheras, Kuala Lumpur, Malaysia; [5]International Medical School, Management and Science University, 40000 Shah Alam, Selangor; [6]Division of Gastroentero-Hepatology, Department of Internal Medicine, Universitas Airlangga, Surabaya, Indonesia

Abstract

Introduction: Vedolizumab (VDZ) is a biologic therapy targeting ulcerative colitis (UC) and Crohn's disease (CD) patients. However, response rates vary, potentially due to intestinal barrier dysfunction. This study aimed to investigate the ultrastructural characteristics and expression of genes related to the intestinal barrier in inflammatory bowel disease patients receiving VDZ therapy. *Materials and Methods:* A prospective cohort study was conducted at Universiti Kebangsaan Malaysia Medical Centre, recruiting UC and CD patients treated with VDZ, with follow-up at 6 months. Colonic biopsies were taken from responders and non-responders, alongside 10 healthy controls for comparison. Messenger RNA levels of *MUC1, CLDN8*, and *OCLN* were quantified using qPCR. Tissue sections were examined for tight junctions, gap junctions, and desmosomes using transmission electron microscopy. Barrier permeability was tested through barrier assay using a nano silver particle translocation assay, and the findings were analysed using inductively coupled plasma-mass spectrometry (ICP-MS). *Results:* Among the 25 patients (14 UC, 11 CD), responders showed significantly increase in *CLDN8* and *MUC1* expressions, while reduced *OCLN* expression compared to non-responders. Non-responders had wider tight and gap junctions. Additionally, responders displayed lower nano silver particle permeability than non-responders and healthy controls. *Conclusion:* Intestinal barrier dysfunction, evidenced by differential intestinal barrier gene expression and ultrastructural alterations, may contribute to the lack of response to VDZ therapy, particularly in biological-naïve CD patients. These findings underscore the critical role of intestinal barrier integrity in therapeutic responsiveness to VDZ in IBD patients.

Keywords: inflammatory bowel disease, ulcerative colitis, intestinal barrier, vedolizumab

INTRODUCTION

Inflammatory bowel disease (IBD) encompasses Crohn's disease (CD) and ulcerative colitis (UC), both characterised by chronic, relapsing inflammation of the gastrointestinal tract.[1] These conditions significantly impact patients' physical and psychological well-being, leading to a reduced quality of life.[2] Despite substantial research efforts, the exact cause of IBD remains unclear. However, it is widely accepted that IBD develops from a complex interaction of genetic susceptibility, environmental factors, immune dysregulation, and gut barrier dysfunction.[3] Among these factors, gut barrier dysfunction has received growing attention due to its potential role in disease progression, treatment response, and long-term prognosis.

The intestinal barrier is composed of a monolayer of epithelial cells held together

*Address for correspondence: Norfilza Mohd Mokhtar. International Medical School, Management and Science University, 40000 Shah Alam, Selangor, Malaysia Tel: +603-5521 6713 (NMM); Email: *norfilza@msu.edu.my*

by tight junctions (TJs), which regulate permeability, maintain mucosal integrity, and prevent the translocation of luminal antigens, toxins, and microbial products. Key components of this barrier include mucins, the outermost layer which form a protective mucus layer over the epithelium; claudins, the middle layer, a family of tight junction proteins that selectively control paracellular permeability; and occludin, the innermost layer, a structural protein essential for tight junction stability.[4,5] Disruption of these components leads to increased intestinal permeability which often described as a "leaky gut" by allowing luminal antigens to penetrate the underlying tissue and trigger excessive immune responses. This chronic immune activation can sustain inflammation, exacerbate tissue damage, and increase disease progression. Research has shown that patients with IBD often exhibit altered expression of these proteins, suggesting compromised barrier function that may influence disease severity and treatment outcomes.[4]

Vedolizumab (VDZ) is a gut-selective anti-integrin biologic that targets α4β7 integrin, reducing lymphocyte trafficking to the gut and minimising inflammation.[6] While VDZ has demonstrated effectiveness in achieving and maintaining remission in a significant proportion of IBD patients, about 40% of patients do not respond to induction therapy, and some experience a loss of treatment response over time.[7] The factors contributing to this variability are not fully understood, but the integrity of the intestinal barrier is believed to be a critical factor influencing therapeutic outcomes.

As the incidence of IBD continues to rise in Malaysia, the use of VDZ as a treatment option is also on the rise as they offer an alternative for patients who may not respond well to conventional treatments or who experience significant side effects.[8] Unlike other biologics that target systemic inflammatory pathways, VDZ has fewer systemic side effects.[9] Furthermore, the treatment approach for IBD typically follows a strategy, starting with conventional therapies for mild cases and progressing to advanced options like biologics for more severe or treatment-resistant cases.[8] Since patients who receive VDZ have often failed to respond to lower-tier treatments, understanding the mechanisms behind VDZ responsiveness is crucial. Identifying factors that influence treatment outcomes could help optimise patient management and improve the effectiveness of IBD therapy.

Given the significant role of the intestinal barrier in IBD pathogenesis and treatment response, this study aims to assess the ultrastructural characteristics and expression of genes related to the intestinal barrier in IBD patients receiving VDZ therapy. By examining the relationship between gut barrier integrity and treatment outcomes, we hope to gain valuable insights into the mechanisms underlying VDZ resistance. This understanding could help predict treatment responses, enhance patient stratification, and optimise individualised treatment strategies for individuals with IBD.

MATERIALS AND METHODS

Clinical Samples

The study cohort was approved by the Research Ethics Committee of Universiti Kebangsaan Malaysia (reference number: UKM/PPI/111/8/JEP-2021-516). The study protocol was also approved by the institutional ethical committee. After obtaining written consent, 25 IBD patients (14 UC, 11 CD) were recruited at the Universiti Kebangsaan Malaysia Medical Centre in Kuala Lumpur. The inclusion criteria include patients diagnosed with IBD and aged between 18 to 60 years old. This range was selected to maintain a more homogenous adult-onset cohort. Also, to avoid the distinct clinical and genetic phenotypes associated with pediatric and very early onset IBD. By limiting the age to 60, we want to exclude elderly-onset IBD, which is frequently associated with complications. Pregnant women, those with irritable bowel syndrome, and IBD patients with any other chronic illnesses were excluded. All recruited IBD patients were on a single biologic agent, VDZ therapy for a minimum of six months. The treatment duration across the cohort ranged from 6 to 48 months. Patients were corticosteroid free of at least six weeks prior to recruitment and received no further steroid during the period of the study.

The Simple Clinical Colitis Activity Index (SCCAI) and the Harvey-Bradshaw Index (HBI) were used to assess disease activity indices for UC and CD, respectively.[10,11] Sixth month post-VDZ therapy, all recruited IBD patients were followed up and underwent colonoscopy procedure to assess endoscopic mucosal healing along with serum C-reactive protein and assessment for SCCAI and HBI. Patients who responded to VDZ therapy at six months were defined as those who demonstrated improvement in clinical symptoms, assessed by SCCAI and HBI scores, along with mucosal healing was assessed using established endoscopic scoring systems. For patients with

UC, the Mayo Endoscopic Subscore (MES) was used to evaluate mucosal inflammation during colonoscopy. Mucosal healing was defined as MES of zero, consistent with partial or complete endoscopic remission (normal or inactive disease).[12] For patients with CD, the Simple Endoscopic Score for Crohn's Disease (SES-CD) was used, which assesses ulcer size, ulcerated surface, affected surface, and presence of strictures across five intestinal segments.[13] Endoscopic remissions in CD were defined as an SES-CD score of <3, or the absence of mucosal ulcers. All endoscopic evaluations were performed by experienced gastroenterologists blinded to treatment response, and scoring was based on the most severely affected segment, a reduction in serum C-reactive protein levels and achievement of endoscopic mucosal healing. All endoscopic assessments were performed at timepoint, e.g., week 24 or 48 to evaluate the long-term response to VDZ. During colonoscopy procedures, colonic biopsies were obtained from inflamed and healed areas in IBD patients and sections stained with hematoxylin and eosin (H&E) were examined to assess the degree of inflammation. The biopsies were stored at -80°C in RNAlater (Sigma Aldrich, St. Louis, MO, USA) until further analysis. Ten normal colorectal tissues were obtained as controls. These samples underwent thorough screening to ensure they were non-inflammatory (free from any active or chronic inflammation) and non-malignant (devoid of any cancerous changes), ensuring they accurately represent healthy tissue. The collection and use of these samples were conducted in compliance with ethical standards, with informed consent obtained from all donors. Brennan *et al.*[14] and the Geboes histological index[15] were used to assess the severity and extent of inflammation in the colon in patients with UC and CD, respectively.

Total RNA Extraction and Quality Assessment

Total RNA was extracted from 46 fresh-frozen biopsy tissues, including 25 pre-treatment samples, 11 post-treatment samples and 10 normal samples, using the AllPrep DNA/RNA/miRNA Universal Kit (Qiagen, Valencia, CA, USA) and QIAshredder columns (Qiagen, Hilden, Germany), according to the manufacturer's protocol. The RNA concentration was determined using a DeNovix DS11+ Spectrophotometer (DeNovix Inc., Wilmington, DE, USA). The quality of the isolated RNA was assessed using agarose gel electrophoresis. The Quantitect Reverse Transcription Kit (Qiagen, Hilden, Germany) was used to convert approximately 1000 ng of total cellular RNA samples to cDNA for quantitative PCR analysis (qPCR).

Quantitative PCR Analysis (qPCR) of Intestinal Barrier Genes

MUC1, CLDN8, and OCLN were selected for qPCR validation. The analysis was performed using the SYBR Green technology, Bio-Rad CFX96 (Bio-Rad Laboratories, CA, USA). Glycerin-aldehyde-3-phosphate (GAPDH) was employed as a housekeeping gene. The primer sequences are summarised in Table 1.

The expression of each inflammatory cytokine was assessed relative to the housekeeping gene *GAPDH*. Primers were designed using Primer Express software version 3.0 and utilised at validated concentrations. These genes' primers were designed commercially by Qiagen, Hilden, Germany, which were then coated on 96-well plates. The final concentration for each primer

Table 1: List of mRNA primer sequences for studied genes

Gene Description	Gene ID	NCBI Code	Length (bp)
MUC1 - *[Homo sapiens]*	4582	NM_002456	125
OCLN - *[Homo sapiens]*	100506658	NM_002538	95
CLDN8 -*[Homo sapiens]*	9073	NM_199328	104
GAPDH (glyceraldehyde-3-phosphate dehydrogenase) *[Homo Sapiens]*	2597	NM_002046	88

was standardised at 100 nM. For qPCR, 2× Quantinova SYBR Green PCR Master Mix, 2 µL Applied Biosystems QN ROX Reference Dye, 2 µL primers and 1 µL of cDNA were added to a 20 µL final volume. The following cycling conditions were used for amplification: 2 min at 95°C, 5 s at 95°C, and 39 two-step cycles of 5 s at 95°C and 10s at 60°C. The threshold cycle (CT/Ct) values obtained by running each sample in triplicate were averaged. The $2^{-\Delta\Delta Ct}$ method was used to analyse relative gene expression.[16]

Transmission Electron Microscopy Sample Preparation and Examination

Eighteen fresh biopsy samples, six samples each for pre-treatment, post-treatment and normal conditions were processed for the transmission electron microscopy at the Department of Diagnostic Laboratory Services, University Kebangsaan Malaysia Medical Centre (UKMMC). Tissue sections were evaluated, and images were captured using an optical microscope (Leica DM1000, Leica, USA). After fixation in 3% glutaraldehyde, the samples were processed using a Leica tissue processor (EM TP, Leica, USA). Briefly, the samples were immersed in 0.1 M phosphate buffer saline (PBS) containing 3% glutaraldehyde (Electron Microscopy Sciences, PA, USA) to preserve the ultrastructure of cells and tissues. The samples were then rinsed three times in 0.1 M PBS before fixation in 0.2 M PBS with 1% osmium tetroxide (Electron Microscopy Sciences, PA, USA). The tissue was then washed with 0.1M PBS, followed by two washes with distilled water. The samples were submerged in 3% uranyl acetate (TED PELLA INC, CA, USA) and again washed twice with distilled water. The samples were dehydrated in increasing concentrations of ethanol (SYSTERM, Malaysia®), subsequently infiltrated with resin (Agar Scientific) mixed with acetone in progressively increasing ratios (1:2, 1:1, 3:1), followed by infiltration with absolute resin overnight. The dehydrated samples were then embedded in epoxy resin and cured overnight at 67°C in an MKII Embedding Oven (Agar Scientific, UK). Semithin sections (1 um thick) were prepared using a Leica MZ 6 Ultracut microtome (Leica Biosystems, USA). The sections were mounted on glass slides, stained with toluidine blue, and examined under an optical microscope (Leica DM1000, Leica, USA) to mark the area of interest. To evaluate the mucosal architecture, the histological pattern was evaluated by a trained pathologist. A series of observations on 30 microscopic fields at magnification ranging from 5× to 100× were performed on LM pictures. A qualitative analysis of the crypt morphology of the intestinal barrier was performed. The area of interest was appropriately trimmed, and each sample was cut into an ultrathin section (80-90 nm) using an Ultra 45 diamond knife (DiATOME, USA). Then, ultrathin sections were collected on copper grids with a mesh size of 150 (TED PELLA INC, CA, USA) and stained using the Modified Negative staining method (3% uranyl acetate and Reynold's lead citrate). Next, the observations were carried out using a transmission electron microscope (FEI TECNAI, USA) set up at 120 kV and equipped with a digital camera (AMT CCD, Deben UK Ltd., Suffolk, UK). Junctional complexes (JC) gap width was one of the morphological features taken into consideration during the analysis of digital TEM pictures using ImageJ software. The ultrastructural features of TJ, GJ, and desmosomes were visualised, and gap widths were quantified at magnifications ranging from 100× to 325×. Only TJ, GJ and desmosomes that were precisely longitudinally sectioned were quantified during the ultrastructural examinations performed on ten selected tissue areas. For each type of intercellular junction, at least three values were obtained. The results were presented as mean values and standard deviations.

Barrier Assay Analysis

Six fresh colonic mucosal biopsies (two each for pre-treatment, post-treatment, normal controls) were harvested from the left colon using biopsy forceps. Each biopsy measured approximately two–three mm in diameter, yielding an exposed surface area of roughly ~7 mm^2 (calculated from $\pi \times (1.5\ mm^2)$. Each biopsy was mounted in a custom chamber sized to fit the tissue such that only the apical surface was exposed to the donor compartment. Silicone gel sealed the biopsy edges to prevent lateral leakage and ensure transport occurred solely through the tissue. A gentle hydrostatic column at a height of 10 mm was applied above the apical side to simulate luminal pressure and drive transport consistent with methodologies used in Ussing chamber setups and permeability assays. A 1 mL solution of silver nanoparticles was prepared by mixing 900 µL of filtered water with 100µL of 2 nm nano silver concentrate to achieve a final concentration of 10 µg/mL and added to the custom-designed chamber, which was sterilised via autoclaving and UV exposure. The system was incubated at

37 °C for 24 h and 48 h. To verify tissue integrity, pre-assay controls employed FITC-dextran (4 kDa) permeability testing to confirm barrier integrity. This probe is a widely validated marker in *ex vivo* intestinal permeability assays.[17] Alternatively, transepithelial electrical resistance (TEER) measurements are commonly used in *in vitro* epithelial barrier models to verify monolayer integrity prior to permeability testing.[18] In this study, only biopsies maintaining a TEER value of > 150 Ω·cm² were included. Biopsies showing abnormal permeability or leakage in these controls were excluded. Basolateral samples (1 mL each) collected at 24 h and 48 h were analysed using inductively coupled plasma mass spectrometry (ICP-MS) to quantify silver nanoparticle translocation. Each condition was tested in duplicate, and the mean values were used for analysis, with an intra-assay variability threshold maintained at < 15% CV. These experiments were performed across four independent experiments.

Statistical Analysis

All statistical analyses were performed using SPSS software version 20.0 (SPSS Inc. Chicago, IL, USA). Demographic data are presented as means and standard deviations for the normally distributed data. For non-normally distributed data, the values are presented as medians (IQR) and the mean differences were calculated using the Wilcoxon signed-rank test. Mann-Whitney U test was used to compare the mean reduction between the groups. For the TEM analysis, the Kruskal-Wallis test was performed to determine changes in the gap width of the TJ, GJ, and desmosomes. The software used was GraphPad Prism Software (San Diego, CA, USA).

RESULTS

A total of 25 IBD patients, with 14 UC (median age: 34 years) and 11 CD (median age: 26.5 years), were included along with 10 healthy controls. Clinical and demographic details of all IBD patients including Montreal Classification, medications received, disease activity index and serum C-reactive protein prior to biologic therapy were shown in Table 2.

Relative Expression of Intestinal Barrier Genes

Relative Expression of Intestinal Barrier Genes in Pre-Treatment IBD

RT-PCR analysis was performed on three intestinal barrier genes that are related with

Table 2: Clinical and demographic details of all Inflammatory bowel disease (IBD) patients. All data are expressed as n except where indicated in the table. UC, ulcerative colitis; CD, Crohn's disease; n, number. Disease activity indices: Harvey-Bradshaw Index (HBI) and Simple Clinical Colitis Activity Index (SSCAI), at pre-treatment with biologic therapy for a minimum of six months

	UC (n=14)	CD (n=11)	Normal (n=10)
Median age (range)	**34**	**26.5**	**28**
Ethnicity			
Malay	5	2	6
Chinese	4	3	2
Indian	5	6	2
Gender			
Male	5	7	4
Female	9	4	6
Smoking status			
Ex-smoker	-	-	-
Non-smoker	14	11	10
Employment			
Full-time	10	9	8
Part-time	-	-	-
Unemployed	4	2	2
Montreal Classification			
Age at diagnosis			
A1: < 17	-	0	-
A2:17- 40	-	8	-
A3:>40	-	3	-
Location			
Terminal ileum, L1	-	0	-
Colon, L2	-	7	-
Ileo-colon, L3	-	4	-
Upper GI, L4	-	0	-
Behaviour			
Non-stricturing penetrating, B1	-	11	-
Stricturing, B2	-	0	-
Penetrating, B3	-	0	-
Perianal, B4	-	0	-
Severity			
S0: Remission	0	-	-
S1: Mild symptoms	0	-	-
S2: Moderate symptoms	12	-	-
S4: Severe symptoms	2	-	-
Extensity			
Ulcerative proctitis. E1	0	-	-
Left-sided UC, E2	12	-	-
Extensive UC, E3	2	-	-
Medications taken			
Corticosteroids	0	0	-
Mesalazine	8	0	-
Azathioprine	0	3	-
Biologic naïve	13	3	-
Non-biologic naive	1	8	-
Post-operative status	0	1	-
Harvey Bradshaw Index (HBI)- Mean value	-	12	-
Simple Clinical Colitis Activity Index (SCCAI)- Mean value	7	-	-
Serum C-Reactive protein- Mean value (mg/dL)	9	12	-
Family history of IBD	0	0	0

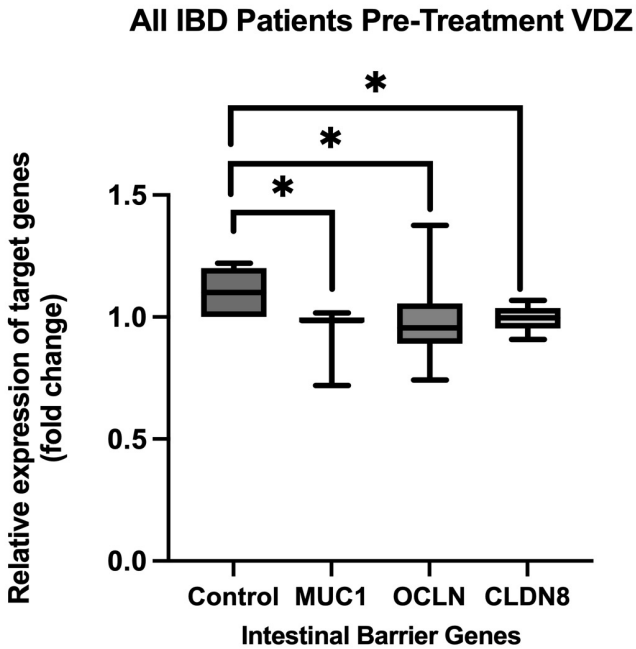

Figure 1. Box plot displaying the relative expression of intestinal barrier genes (MUC1, CLDN8 and OCLN) in pre-treatment Vedolizumab (VDZ) of all Inflammatory bowel disease (IBD) patients. Symbol * represents $p < 0.05$.

IBD namely *MUC1, CLDN8*, and *OCLN*. *MUC1, CLDN8* and *OCLN* expressions were significantly reduced in the pre-treatment VDZ compared to control ($p = 0.0023$) (Figure 1).

At baseline (pre-treatment VDZ), stratification of IBD patients according to subsequent response to VDZ revealed significant differences in intestinal barrier gene expression between future responders and non-responders. Non-responders exhibited significantly lower *CLDN8* and *OCLN* expression together with higher *MUC1* compared with responders, indicating a distinct pre-treatment epithelial barrier profile. In contrast, responders demonstrated lower *CLDN8*, *MUC1* and *OCLN* expression prior to therapy initiation (Figure 2).

Relative Expression of Intestinal Barrier Genes in Post-Treatment VDZ

The expression of two genes, *MUC1* and *CLDN8*, was significantly higher in the post-treatment VDZ of responder IBD compared to both non-responders and the control group ($p < 0.0001$) (Figure 3a and Figure 3b, respectively). On the other hand, *OCLN* expression was significantly reduced in the post-treatment VDZ of responders compared to non-responders and the control group ($p = 0.0004$) (Figure 3c).

Table 3: Comparison of pre- and post-treatment serum C-reactive protein levels between vedolizumab (VDZ) responders and non-responders

	Pre-treatment VDZ (n=11)	Post-treatment VDZ (n=11)	p-Value
Serum C-Reactive protein (Mean value in mg/dL)			
Responders VDZ	10	3	0.0061
Non-responders VDZ	11	10	0.034

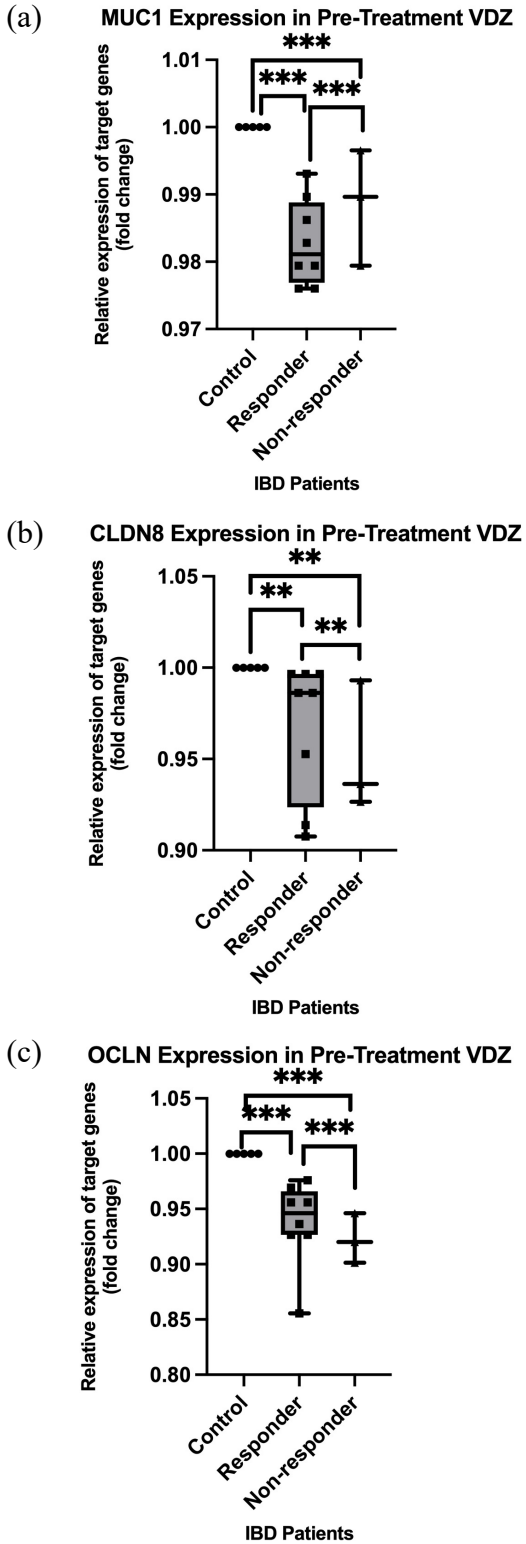

Figure 2. Box plot displaying the relative expression of intestinal barrier genes (*MUC1, CLDN8* and *OCLN*) in pretreatment Vedolizumab (VDZ) (a) Expression of *MUC1* in pre-treatment Inflammatory bowel disease (IBD) patients to VDZ. (b) Expression of *CLDN8* in pre-treatment IBD patients to VDZ. (c) Expression of *OCLN* in pre-treatment IBD patients to VDZ. Symbol ** represents $p < 0.01$, symbol *** represents $p < 0.001$.

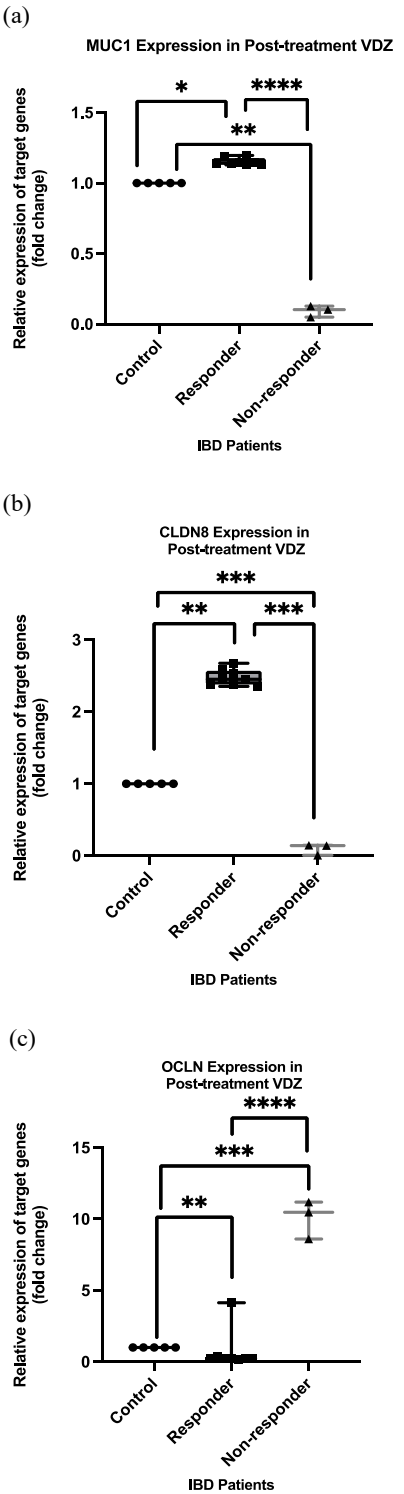

Figure. 3. Box plot displaying the relative expression of intestinal barrier genes (*MUC1, CLDN8* and *OCLN*) in post-treatment VDZ (a) Expression of *MUC1* in post-treatment IBD patients to VDZ. (b) Expression of *CLDN8* in post-treatment IBD patients to VDZ. (c) Expression of *OCLN* in post-treatment IBD patients to VDZ. Symbol * represents $p < 0.05$, symbol ** represents $p < 0.01$, symbol *** represents $p < 0.001$, symbol **** represents $p < 0.0001$.

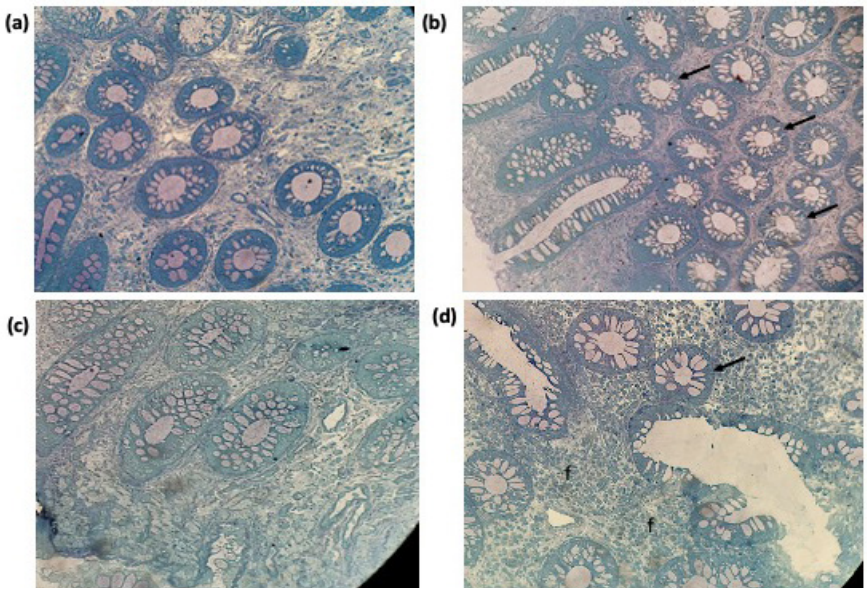

Figure 4. Representative images of Toluidine blue-stained semi-thin sections of colonic biopsy illustrate specific intestinal barrier function from inflammatory bowel disease (IBD) patients. Light microscopy (LM) histological images of intestinal mucosal barrier biopsies in IBD patients. (a) Control (100×) (b) Pre-treatment IBD, chronic colitis with variable diameters in adjacent crypts in a cross section with dilated crypts containing mucus (arrows; 100×) (c) Non-responder VDZ, chronic colitis with high- grade dysplasia (200×) (d) Responder VDZ, longitudinal section with diffuse inflammatory cell infiltrations (f) (100×).

Ultrastructural Features of Apical Junctional Complexes

Light Microscopy Observation

Figure 4 describes the histological features of intestinal mucosal barrier observed under light microscopy.

Transmission Electron Microscopy (TEM) Observations

TEM images of the JC are shown in Figure 4. The groups studied are compared according to each junctional complexes (JC) component (TJ, GJ, and desmosomes) in Figure 5.

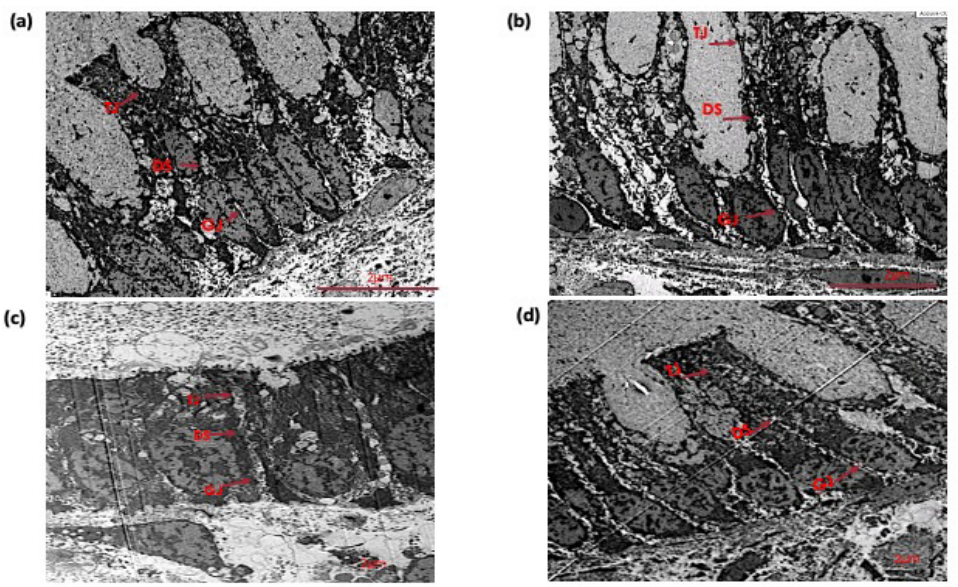

Figure 5. Transmission Electron Microscopy (TEM) images of bowel in IBD (a) Control (b) Pre-treatment IBD (c) Non-responder of post-treatment VDZ (d) Responder of post-treatment VDZ. TJ, tight junction; GJ, gap junction; DS, desmosome.

Notably, the desmosome gap width showed no significant differences among all groups. However, the tight junction (TJ) and gap junction (GJ) width were more dilated in all experimental groups compared to the controls. Specifically, TJ gap width in pre-treatment IBD was found wider as compared to control. In non-responders to VDZ, the post-treatment IBD showed a wider TJ gap compared to both responders and the control (Figure 6a). The desmosome gap width was consistently wider in pre-treatment, responder VDZ, non-responder VDZ and control groups patient but no significant differences were observed these groups. Notably, the widest desmosome gaps were observed in non-responders to VDZ, while the narrowest were in the controls (Figure 6b). An increase in GJ width was also observed in pre-treatment IBD compared to the control group. Additionally, the GJ width in non-responders was wider as compared to both responders and the control group (Figure 6c).

Barrier Assay

The calibration graph of ICP-MS analysis using step mass element, Ag, are shown below in Figure 7.

The amount of nanosilver particles that passed through in the pre-treatment responder VDZ was found higher at 24 hours and 48 hours of treatment compared to control. Conversely, in the post-treatment responder VDZ, the concentration of nanosilver particles that passed through was lower at 24 hours and 48 hours compared to both pre-treatment responder VDZ and the control (Figure 8a). In the non-responder VDZ, the concentration of nanosilver particles that passed through in pre-treatment VDZ were higher at 24 hours and 48 hours compared to the control. On the other hand, in the post-treatment VDZ, the concentration of nanosilver particles that passed through was higher at both 24 hours and 48 hours compared to pre-treatment non-responder VDZ and the control group (Figure 8b).

DISCUSSION

The experimental focus of our current study was to investigate the roles of intestinal barrier function specifically the expression of intestinal barrier genes (*MUC1, CLDN8*, and *OCLN*) in maintaining ultrastructural integrity of this barrier in IBD. The study observed a possible correlation between the lower expression of these transcripts with the physical widening of TJ and GJ complexes. This structural failure is most likely causing increased intestinal permeability that will facilitate the paracellular influx of luminal antigens, aggravating the inflammatory process in IBD. This study mainly highlights the important and novel mechanism for the regulation of *CLDN8* which is critical to intestinal homeostasis through the gap width of junctional complexes of TJ and GJ. The effect of anti-integrin treatments on *CLDN8* expression in IBD patients is an area of ongoing research. Anti-inflammatory therapies, such as biologic agents targeting tumor necrosis factor- alpha (TNF-α), have shown efficacy in reducing inflammation and promoting mucosal healing in IBD patients.[19] Some studies have suggested that these treatments may have an impact on claudin expression and barrier function. CLDN8 is a tight junction protein that has been shown to be involved in the regulation of intestinal permeability. *CLDN8* is also one of the most elevated genes that have been identified as such barrier-determining TJ proteins. TJ proteins (e.g., claudins, occludins, zonula occludens, tricellulin) in the intestine help to form a permeable seal between specialised epithelial cells, which is important in paracellular transport pathways and acts as a physical barrier to pathogens.[20] CLDN8 serves as a sealing claudin in junctional regions of normal epithelium surface as well as crypts; however, the absence of it and redistribution from TJs to cytoplasm may result in TJ structure breakdown and increased epithelial permeability in IBD, particularly in active CD.[21] A study by Zhuang *et al*.[22] has investigated the expression of *CLDN8* in IBD patients. The study has found that *CLDN8* expression was significantly downregulated in IBD patients compared to healthy patients. CLDN8, an essential member of the claudin family, was also significantly downregulated in CD patients and TNBS-induced colitis mice. A significant finding from the study was the downregulation of *CLDN8* expression is associated with intestinal mucosal barrier failure. The authors suggested that the upregulation of *CLDN8* expression may be a mechanism by which anti-integrin therapy is correlated with improved gut barrier function in IBD patients. Another study by Wang *et al*.[23] investigated the expression of *CLDN8* in both IBD patients and mice with experimental colitis. That study found that downregulation of CLDN8 is linked to inflammation-induced intestinal mucosal damage and mucosal healing retardation in both IBD patients and mice with

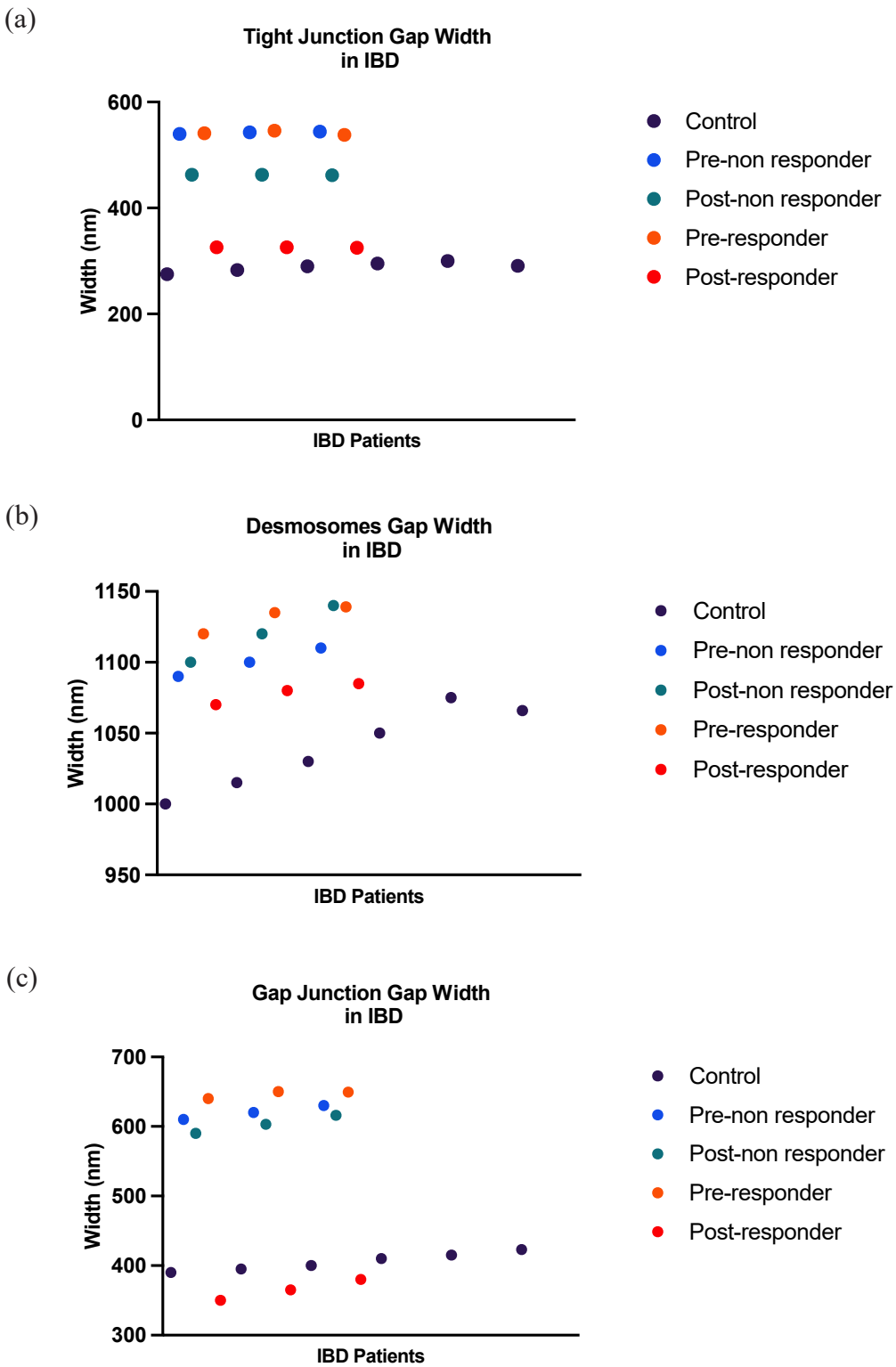

Figure 6. Scatter plot displaying the gap width of junctional complexes (TJ, GJ and desmosomes) of inflammatory bowel disease (IBD) patients. (a) TJ gap width of IBD patients. (b) Desmosomes gap width of IBD patients. (c) GJ gap width of IBD patients.

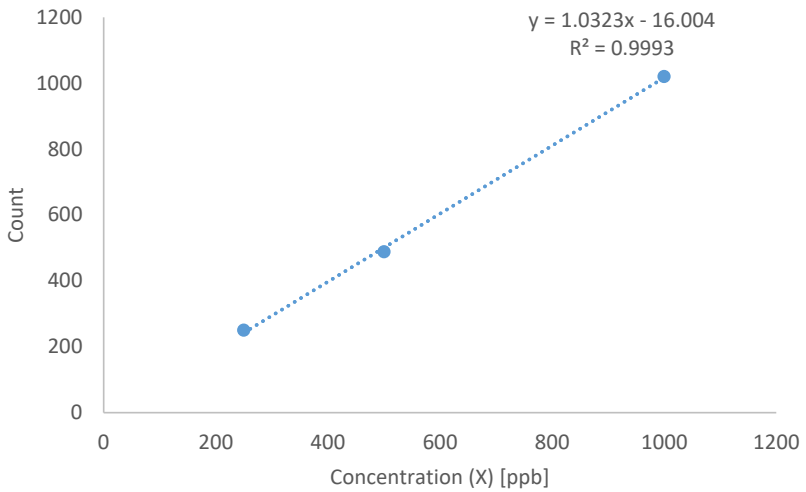

Figure 7. Line graph displaying the calibration graph for coupled plasma-mass spectrometry (ICP-MS) analysis using step mass element, Ag.

experimental colitis.[23] The authors suggested that the upregulation of *CLDN8* expression may be a mechanism potentially underlying how VDZ contributes to gut barrier function improvement in IBD patients.

Interestingly, our study discovered that *CLDN8* and *MUC1* exhibited higher expressions among responders to VDZ in IBD patients, both UC and CD as compared to non-responder. These genes may serve as potential biomarkers for therapeutic success. The involvement of mucins in UC has been minimally explored in the context of UC. Prior study demonstrated that *MUC12* mRNA expression was significantly downregulated in patients with active UC compared with those in remission and healthy controls, and this reduction was associated with disruption of colonic mucosal integrity.[24] On the other hand, *OCLN* expression was significantly reduced in VDZ-responders compared to non-responders. The discrepancy with the work of Yamamoto-Furusho *et al*.,[25] who reported high expression of *OCLN* in active UC compared to UC in remission and healthy control groups. From a clinical perspective, this finding may explain the dynamic role of epithelial barrier during the healing process. During active disease, the upregulation of *OCLN* likely represents a compensatory mechanism in order to repair the barrier defect and maintain cell polarity during acute inflammation.[25] Consequently, the downregulation of *OCLN* may signify a change from this hyper proliferative state to a stabilised, homeostatic mucosal environment. It is important to distinguish these findings with CD, whereby barrier dysfunction is governed by sealing proteins like CLDN5 and CLDN8, and the upregulation of pore-forming tight junction protein CLDN2, reported by Zeissig *et al*.[21] Redistribution of sealing CLDN5 and 8 can lead to altered tight junction structure and pronounced barrier defect in mild to moderately active CD. However, there are insufficient information about differential expressions of intestinal barrier genes in UC or CD and the ultrastructural changes of intestinal barrier function in IBD patients, focusing on VDZ treatment.

Previous study on *in vitro* has also found that altered epithelial claudin expression has influenced the permeability of intestinal epithelial barrier that might lead to barrier defect.[26] Our TEM observations were initially focused on the gap width of the junctional complexes which were TJ, desmosomes and GJ. Alterations in the ultrastructural features include increased gap width of TJ and GJ in non-responder IBD patients, particularly CD patients treated with VDZ. Changes in TJ function and TJ-protein expression in IBD have attracted significant scientific attention, as increased intestinal epithelial permeability is a key hallmark of IBD. Interestingly, this barrier dysfunction can occur even before the onset of overt inflammation.[27,28] Additionally, the loss of mucosal epithelial TJ proteins may facilitate epithelial leakage and activates mucosal immune responses.[29] On the

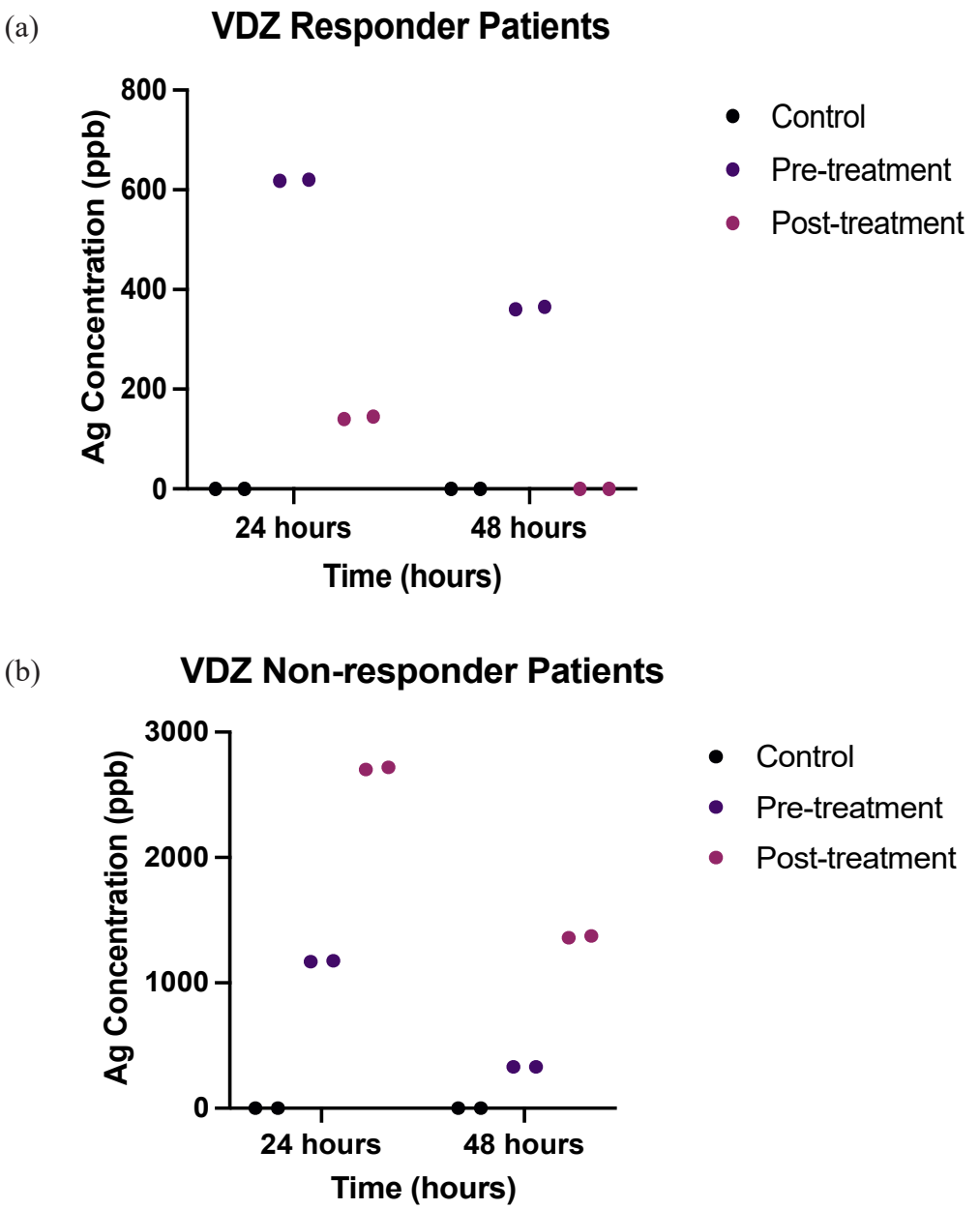

Figure 8. Scatter plot displaying the concentration of nanosilver particles of inflammatory bowel disease (IBD) patients (a) The concentration of nanosilver particles in responder VDZ (b) The concentration of nanosilver particles in non-responder VDZ.

other hand, our study has found that the largest gap between the desmosomes were observed not only in controls and VDZ-treated cohorts (responders and non-responders). Although VDZ non-responders showed a trend toward increased spacing, no statistically significant differences were observed between the groups pre-treatments. Our data showed a positive response to VDZ specifically biological naïve UC patients, that was associated with a decreased in the gap width of TJ and GJ. This structural reinforcement strongly correlates with the upregulated expression of *CLDN8*. A study by Angelow *et al*.[30] indicates that CLDN -1, -3, -4, -5, and -8 decrease paracellular permeability of the intestine, whereas claudin-2 forms cation-selective channels that increase paracellular NaCl and water reabsorption, thereby reducing

transepithelial permeability. They showed that high expression of *CLDN8* and thus correlated with alteration in the permeability of the intestine, suggesting that *CLDN8* may play a crucial role in the intestinal barrier of IBD patients. As a result, it is not surprising that we found *CLDN8* downregulation of non- responder IBD to VDZ in our study as it can be associated with altered ultrastructural features of the intestinal barrier function by reducing the gap width of TJ and GJ. Wider TJ and GJ can lead to an increased permeability of the intestinal barrier function. This can also be supported by a higher concentration of nano silver particles of non-responder VDZ in our study which indicated an increased permeability of intestinal barrier function or 'leaky gut'.

There were a few limitations in this study. The sample size for the study was relatively small and may have led to a high probability of Type I statistical errors and a higher chance of confounding factors affecting the results. Moreover, this is a single-center study and thus the number of patients in each arm was limited. Most likely, it was due to our stringent inclusion and exclusion criteria. We were also actively cautious in selecting the potential IBD patients who would be only on VDZ treatment, as data filtering was conducted based only the mentioned biological treatment, VDZ. This study fills an existing gap through the fundamental role of CLDN8 in altering the gap width of junctional complexes and thus highlighting the complex role of the mechanisms in intestinal homeostasis. Hence, this may offer a new perspective on the expression of intestinal barrier genes and the significance of restoring mucosal barrier function, thus prevention of the intestinal barrier dysfunction in patients with IBD. Through our findings, we successfully identified that IBD patients, in particular CD who were non-responsive to VDZ treatment exhibited a downregulation of CLDN8 expression and demonstrated wider TJ and GJ gap width that potentially responsible for the leaky gut in IBD. This could serve as the foundation not only for studying specific changes that lead to non-responsive towards VDZ treatment, but also the changes in ultrastructural features of intestinal barrier function that may lead to leaky gut in IBD. A recent study by Kato *et al*.[31] and Borisova *et al*.[32] has stated that a variety of systemic diseases are included under the term "leaky gut syndrome". They found that leaky gut syndrome may have an association between LGS and gastrointestinal and non-GI diseases such as inflammatory bowel disease, irritable bowel syndrome (IBS), colorectal cancer (CRC), allergies, Huntington's disease, and Parkinson disease.[33,34] In addition, translocation of microorganisms and their toxic metabolites beyond the gastrointestinal tract is one of the fallouts of the leaky gut.[35] A study by Teodora *et al*. (2016) also has showed that patients with CD who failed to respond to VDZ had significantly higher levels of intestinal permeability compared to patients who responded to the drug.[36]

This finding offers a new perspective on tackling intestinal barrier function for the future effective treatment of IBD. To further explore the changes in intestinal barrier function with disease development on VDZ treatment, more studies might be conducted by enlisting a broader patient group covering various disease durations, such as at 5 to 7-year intervals. IBD patients, in particular CD, who were non-responsive to VDZ treatment exhibited a downregulation of *CLDN8* expression and demonstrated wider TJ and GJ gap width that potentially responsible for the leaky gut in IBD. We suggested that the increase in TJ and GJ gap width may be a mechanism by which *CLDN8* expression impaired gut barrier function in responder to VDZ patients. Translocation of microorganisms and their toxic metabolites beyond the gastrointestinal tract is one of the fallouts of the leaky gut. This finding offers a new perspective on tackling intestinal barrier function for the future effective treatment of IBD.

CONCLUSION

These data imply that VDZ responsiveness in IBD patients may be significantly influenced by the expression of *CLDN8* and *MUC1*, as well as the gap widths of TJ and GJ. The restoration of intestinal barrier function by VDZ may be aided by changes in these variables.

Acknowledgements: We would like to thank the staff from the Gastroenterology Unit, UKMMC and the Department of Physiology, UKM for their assistance and coordination with biospecimen collection. This research was funded by the Fundamental Research Grant Scheme, Ministry of Higher Education, Malaysia (FRGS/1/2020/SKK0/UKM/01/2).

Informed Consent Statement: Informed consent was obtained from all studied subjects in the study.

Authors' contributions: All authors have made a significant contribution to the research described in this manuscript. N.M.M and R.A.R.A; methodology and participant recruitments, N.M.M, R.A.R.A, and N.A.S; validation, G.C.T and N.M.M; data analysis, N.A.S and N.M.M; writing—original draft preparation, N.A.S; writing—review and editing, N.M.M and R.A.R.A; supervision, N.M.M and R.A.R.A. All authors have read and agreed to the published version of the manuscript.

Conflicts of Interest: The authors declare no conflict of interest.

REFERENCES

1. Peyrin-Biroulet L, Panés J, Sandborn WJ, *et al*. Defining disease severity in inflammatory bowel diseases: current and future directions. Clin Gastroenterol Hepatol 2016;14(3):348-354.e17.
2. Jones JL, Nguyen GC, Benchimol EI, *et al*. The impact of inflammatory bowel disease in Canada 2018: quality of life. J Can Assoc Gastroenterol 2019;2(Suppl 1):S42-S48.
3. Ananthakrishnan AN, Bernstein CN, Iliopoulos D, *et al*. Environmental triggers in IBD: a review of progress and evidence. Nat Rev Gastroenterol Hepatol 2018;15(1):39-49.
4. Groschwitz KR, Hogan SP. Intestinal barrier function: molecular regulation and disease pathogenesis. J Allergy Clin Immunol 2009;124(1):3-20.
5. Breugelmans T, Oosterlinck B, Arras W, *et al*. The role of mucins in gastrointestinal barrier function during health and disease. Lancet Gastroenterol Hepatol 2022;7(5):455-471.
6. Lam MC, Bressler B. Vedolizumab for ulcerative colitis and Crohn's disease: results and implications of GEMINI studies. Immunotherapy 2014;6(9):963-971.
7. Zingone F, Barberio B, Compostella F, *et al*. Good efficacy and safety of vedolizumab in Crohn's disease and ulcerative colitis in a real-world scenario. Ther Adv Gastroenterol 2020;13:1756284820936536.
8. Mokhtar NM, Nawawi KNM, Verasingam J, *et al*. A four-decade analysis of the incidence trends, sociodemographic and clinical characteristics of inflammatory bowel disease patients at single tertiary centre, Kuala Lumpur, Malaysia. BMC Public Health 2019;19:1-10.
9. Vermeire S, Loftus EV Jr, Colombel JF, *et al*. Long-term efficacy of vedolizumab for Crohn's disease. J Crohns Colitis 2017;11(4):412-424.
10. Walmsley R, Ayres R, Pounder R, *et al*. A simple clinical colitis activity index. Gut 1998;43(1):29-32.
11. Harvey R, Bradshaw J. A simple index of Crohn's disease activity. Lancet 1980;315(8167):514.
12. Schroeder KW, Tremaine WJ, Ilstrup DM. Coated oral 5-aminosalicylic acid therapy for mildly to moderately active ulcerative colitis. N Engl J Med 1987;317(26):1625-1629.
13. Daperno M, D'Haens G, Van Assche G, *et al*. Development and validation of a new, simplified endoscopic activity score for Crohn's disease: the SES-CD. Gastrointest Endosc 2004;60(4):505-512.
14. Brennan GT, Melton SD, Spechler SJ, *et al*. Clinical implications of histologic abnormalities in ileocolonic biopsies of patients with Crohn's disease in remission. J Clin Gastroenterol 2017;51(1):43-48.
15. Geboes K, Riddell R, Öst A, *et al*. A reproducible grading scale for histological assessment of inflammation in ulcerative colitis. Gut 2000;47(3):404-409.
16. Livak KJ, Schmittgen TD. Analysis of relative gene expression data using real-time quantitative PCR and the $2^{-\Delta\Delta CT}$ method. Methods 2001;25(4):402-408.
17. Schoultz I, Keita ÅV. The intestinal barrier and current techniques for the assessment of gut permeability. Cells 2020;9(8):1909.
18. Williams KM, Gokulan K, Cerniglia CE, *et al*. Size and dose dependent effects of silver nanoparticle exposure on intestinal permeability in an in vitro model of the human gut epithelium. J Nanobiotechnology 2016;14(1):62.
19. Gareb B, Otten AT, Frijlink HW, *et al*. Local tumor necrosis factor-α inhibition in inflammatory bowel disease. Pharmaceutics 2020;12(6):539.
20. Lee B, Moon KM, Kim CY. Tight junction in the intestinal epithelium: its association with diseases and regulation by phytochemicals. J Immunol Res 2018;2018:2645465.
21. Zeissig S, Bürgel N, Günzel D, *et al*. Changes in expression and distribution of claudin 2, 5 and 8 lead to discontinuous tight junctions and barrier dysfunction in active Crohn's disease. Gut 2007;56(1):61-72.
22. Zhuang X, Chen B, Huang S, *et al*. Hypermethylation of miR-145 promoter-mediated SOX9-CLDN8 pathway regulates intestinal mucosal barrier in Crohn's disease. EBioMedicine 2022;76.
23. Wang H, Chao K, Ng SC, *et al*. Pro-inflammatory miR-223 mediates the cross-talk between the IL23 pathway and the intestinal barrier in inflammatory bowel disease. Genome Biol 2016;17:1-15.
24. Yamamoto-Furusho JK, Ascaño-Gutiérrez I, Furuzawa-Carballeda J, *et al*. Differential expression of MUC12, MUC16 and MUC20 in patients with active and remission ulcerative colitis. Mediators Inflamm 2015;2015:659018.
25. Yamamoto-Furusho JK, Mendivil-Rangel EJ, Fonseca-Camarillo G. Differential expression of occludin in patients with ulcerative colitis and healthy controls. Inflamm Bowel Dis 2012;18(10):E1999.
26. Albert-Bayo M, Paracuellos I, González-Castro AM, *et al*. Intestinal mucosal mast cells: key modulators of barrier function and homeostasis. Cells 2019;8(2):135.
27. Mo J, Ni J, Zhang M, *et al*. Mulberry anthocyanins ameliorate DSS-induced ulcerative colitis by improving intestinal barrier function and modulating gut microbiota. Antioxidants (Basel) 2022;11(9):1674.
28. Chelakkot C, Choi Y, Kim DK, *et al*. Akkermansia muciniphila-derived extracellular vesicles influence

gut permeability through the regulation of tight junctions. Exp Mol Med 2018;50(2):e450.
29. Landy J, Ronde E, English N, *et al*. Tight junctions in inflammatory bowel diseases and inflammatory bowel disease associated colorectal cancer. World J Gastroenterol 2016;22(11):3117.
30. Angelow S, Alan S. Structure-function studies of claudin extracellular domains by cysteine-scanning mutagenesis. J Biol Chem 2009;284(42):29205-29217.
31. Kato T, Honda Y, Kurita Y, *et al*. Lubiprostone improves intestinal permeability in humans, a novel therapy for the leaky gut: a prospective randomized pilot study in healthy volunteers. PLoS One 2017;12(4):e0175626.
32. Borisova MA, Achasova KM, Morozova KN, *et al*. Mucin-2 knockout is a model of intercellular junction defects, mitochondrial damage and ATP depletion in the intestinal epithelium. Sci Rep 2020;10(1):21135.
33. Mohamad Nor MH, Ayob N, Mokhtar NM, *et al*. The effect of probiotics (MCP® BCMC® strains) on hepatic steatosis, small intestinal mucosal immune function, and intestinal barrier in patients with non-alcoholic fatty liver disease. Nutrients 2021;13(9):3192.
34. Truta B, Begum F, Datta LW, *et al*. Inflammatory bowel diseases before and after 1990. Gastro Hep Adv 2023;2(1):22-32.
35. Twardowska A, Makaro A, Binienda A, *et al*. Preventing bacterial translocation in patients with leaky gut syndrome: nutrition and pharmacological treatment options. Int J Mol Sci 2022;23(6):3204.
36. Manuc TE, Manuc MM, Diculescu MM. Recent insights into the molecular pathogenesis of Crohn's disease: a review of emerging therapeutic targets. Clin Exp Gastroenterol 2016;9:59-70.